Adaptive optics dioptric scanning ophthalmoscope with a wider field of view similar to those of normal ophthalmoscopes

Tatsuo Yamaguchi,[1] Toshifumi Mihashi,[1,2,]* Yoshiyuki Kitaguchi,[2] Hiroyuki Kanda,[2] Takeshi Morimoto,[2] and Takashi Fujikado[2]

[1]*Optics Lab, Topcon Corp., 75-1Hasunumacho, Itabashi, 174-8580, Japan*

[2]*Applied Visual Science Department, Osaka University Graduate School of Medicine, 2-2 Yamadaoka, Suita, 565-0871, Japan*

Corresponding author: tmihashi@live.jp

We introduce a newly developed adaptive optics dioptric scanning ophthalmoscope (AO-DSO) in which all powered optical parts were refractive lenses instead of concave or convex mirrors. By designing dioptric optics, we were able to achieve a compact instrument with a 10 deg field of view (FOV10) and 1.5 deg field of view (FOV1.5) high-resolution imaging. Although the resolution of FOV10 was sacrificed because of the variation of aberrations of the eye over the 10 deg field, our system works with AO in the case of FOV1.5 and can be used as a scanning laser ophthalmoscope with good optical slicing in the case of FOV10. To test the ability of the AO-DSO, we performed imaging on a normal subject and on a patient with occult macular dystrophy.   © 2012 Optical Society of America

OCIS codes: 170.5755, 330.4460.

Soon after the invention of the adaptive optics ophthalmoscope [1], a scanning version of the ophthalmoscope was introduced [2]. Since then, the adaptive optics scanning laser ophthalmoscope (AO-SLO) has been heavily and successfully used in many productive studies [3]. The instrumentation of the AO-SLO has been improved with modern, sophisticated technologies. It has been equipped with a retinal tracker to compensate for eye movement, optics that observe a wide field of view (FOV) [4], and spectral domain optical coherence tomography [5]. An advanced system can even resolve rod photoreceptors [6]. Another trend has been the development of practically useful clinical instruments from inexpensive devices, such as line scan mechanisms [7] or microelectro mechanical systems (MEMS) mirrors [8].

To our knowledge, most AO-SLOs are built with reflective concave and convex mirrors. Some of them use refractive lenses, but some optical elements are still reflective because the use of refractive elements can cause unwanted reflections, which eventually become noise in wavefront sensor and retinal images. One limitation of reflex concave and convex mirrors is that they reduce aberrations over a small FOV.

We have built an adaptive optics dioptric scanning ophthalmoscope (AO-DSO) without using any concave or convex mirrors; instead, we used refractive lenses for all of the power optics. One of our interests was developing small and simplified AO scanning ophthalmoscopes for clinical needs. The obstacles to their clinical use are their high cost, large size, limited clinical applications, and small FOV. The device typically responsible for the high cost is the deformable mirror. However, we believe that the price of deformable mirrors is decreasing with advances in MEMS technology.

The optics of the AO-DSO introduced in this study had an area of 400×450 mm. The AO-DSO is smaller than a commercially available ophthalmoscope (TRC-50LX, Topcon, Tokyo, Japan), which has an area of 505×506 mm. Using the advantages of dioptric optics, we designed and built an AO scanning system with a high-resolution 0.92×1.25 deg FOV (FOV1.5), a medium resolution 1.8×2.6 deg FOV (FOV3), and a normal scanning system with a 6.9×9.6 deg FOV (FOV10). The maximum FOV was determined by an objective lens, for which we used an objective lens from a commercially available autorefractometer (KR8100, Topcon, Tokyo, Japan).

Using the AO-DSO, we investigated images with FOV1.5 and FOV10 on normal eyes and eyes with occult macular dystrophy (OMD). We also investigated imaging of the nerve fiber layer (NFL) and photoreceptor layer. Additionally, one important concern addressed here is the effectiveness of the AO for FOV10 and FOV1.5 images.

A schematic of the AO-DSO optics is shown in Fig. 1. The light source for the imaging and wavefront sensing was an 840 nm superluminescent diode (SLD, AS8E210GP30M, Anritsu, Kanagawa, Japan). The spectral half width of the SLD was 15 nm. The radiant power at the cornea was 80 μW. The beam diameter at the pupil was 6 mm. If optics are diffraction limited, the optical resolution is 0.58 arcmin. Our system was designed so that FOV1.5 is diffractive limited for the 740–1000 nm spectral region and for the vergence range from –5 to +5 D. The SLD was coupled with a single-mode optical fiber, and the light emitted from the fiber impinged on a deformable mirror (Mirao 52d, Imagine Eyes, Orsay, France), a vertical scanner, and then a horizontal scanner. The deformable mirror and scanners were optically conjugated with the pupil of the eye. The vertical scan was driven by a galvanic scanner (VM2500+, Cambridge Technology, Lexington, Massachusetts), and the horizontal scan was driven by an 8 kHz resonant scanner (8 kHz CRS, Cambridge Technology, Lexington, Massachusetts). The vertical and horizontal scanners can change the scanning range of the retina from 0.92 to 6.9 deg and from 1.25 to 9.6 deg, respectively. After the scanners, the light passed through a focusing prism and objective lens to the retina.
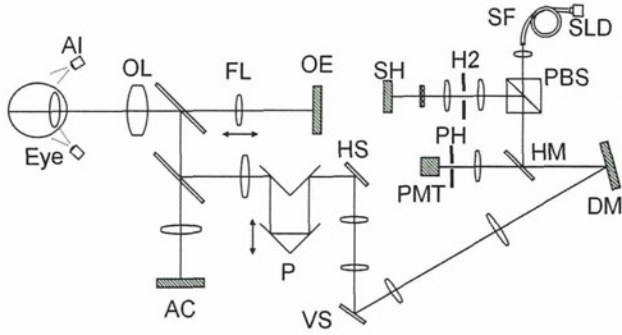
Fig. 1.   AI, light source for imaging the anterior part of the eye; OL, objective lens; FL, focusing lens; OE, organic electroluminescence diode display; AC, CCD for anterior imaging; P, focusing prism; HS, horizontal scanner; VS, vertical scanner; DM, deformable mirror; PBS, polarized beam splitter; HM, half-mirror; PH, pinhole; H2, 2 mm diameter hole; PMT, photomultiplier; SH, Shack–Hartmann wavefront sensor; SF, single mode fiber; SLD, superluminescent diode. Most lenses are doublet-type lenses.

An anti-reflection (AR) coating was applied to all of the refractive lenses' surfaces, and the reflectance after the coating was less than 0.02% at 840 nm (Fig. 2). The AR coating was developed especially for our wavefront sensor product (KR-1W, Topcon, Tokyo, Japan) using ion-assisted deposition technology. We used the focusing prism to correct the spherical errors (−5 to +5D) of the eyes, such that the retina and optical fiber were optically conjugated. The reflected light from the retina was passed from the retina to the deformable mirror. After the deformable mirror, the light reached a photomultiplier (PMT; H7732-10, Hamamatsu Photonics, Hamamatsu, Japan) for imaging. The sampling rate of the electronic circuit for imaging was 15 MHz. The pixel number of the image was 500×700. The acquisition frame rate was 30 frames per second. Scanning ranges were changed for three FOVs. The pixels per arc minute of FOV10, FOV3, and FOV1.5 were 0.83, 0.22, and 0.11, respectively. The ratio of penetration and reflection of a half-mirror after the deformable mirror was 9 to 1 because the light returned from the retina should retain as much of its intensity as possible. The pinhole in front of the PMT was optically conjugated with the fiber of the light source through the layer of the retina that we wanted to image. The optical magnification between the retina and pinhole was 3.5. The pinhole was five times (17.5 times in real dimensions) as large as the Airy disk. Ten percent of the light reflected at the half-mirror went to a polarized beam splitter (PBS), and then polarized light went to a Shack—Hartmann wavefront sensor (SHWS). The PBS was used to form cross-polarized isolation blocking noise light from optics of the instrument and eye to the SHWS. We also inserted a
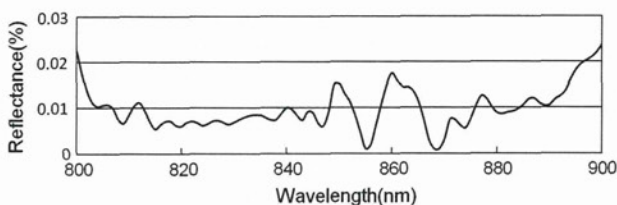

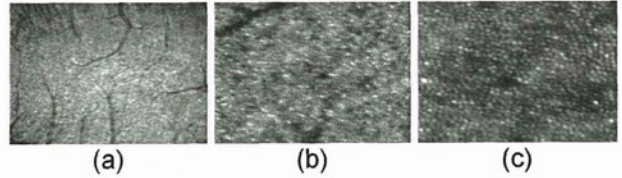Fig. 2.   Anti-reflection coating of the objective lens.

Fig. 3.   Imaging of the photoreceptor layer of a normal retina at three different magnifications. The images were taken at 5 deg nasal from the fovea. All the images were obtained by averaging 10 images. (a) FOV10, (b) FOV3, and (c) FOV1.5.

2 mm diameter hole in front of the SHWS, which is optically conjugated with the retina. This tactic effectively blocks reflection noise from the anterior part of the eye.

The SHWS consisted of a lens array and charge coupled device (CCD). The image obtained by the CCD was analyzed with Zernike polynomials. The coefficients from the second-to sixth-order terms were sent to the control circuit of the deformable mirror to compensate for eye aberrations. Two 940 nm light emitting diodes and a CCD were used to image the anterior part of the eye. An organic electroluminescent diode display (OELD) was used for the fixation target.

The eyes of the subjects were dilated before imaging. Using an electrically adjustable chin rest and the image of the anterior part of the eye, the center of the pupil was aligned to the optical axis of the objective lens of the AO-DSO. The focusing prism for imaging and the focusing lens for the fixation target were adjusted to correct for the eye's spherical error. The OELD fixation target was shown at a certain position on the OELD to rotate the eye, allowing any desired position of the retina within 5 deg from the fovea to be imaged. After the alignment was completed, the imaging SLD was turned on to begin imaging. The focusing prism was precisely controlled to image a particular layer of the retina. The feedback loop of the wavefront sensing and compensation was 10 Hz. The protocol for this study was approved by the Institutional Review Board (IRB) of the Osaka University Medical School, and the procedures conformed to the tenets of the Declaration of Helsinki.

We performed imaging on the eye of a normal male (36 years old) and on an eye with OMD. We confirmed
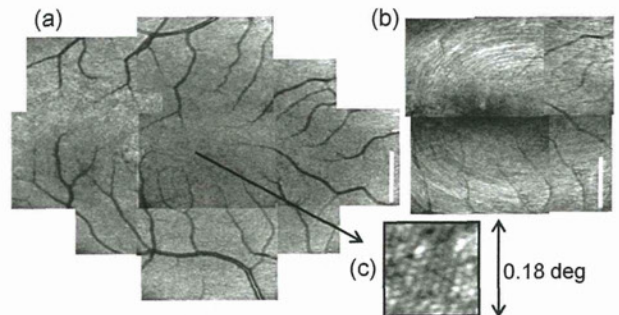

Fig. 4.   Optical sectioning between retinal photoreceptor layers and nerve fiber layers. (a) A montage FOV10 image of the photoreceptor layer. (b) A montage FOV10 image of the nerve fiber layer. The white bar represents 3.5 deg. (c) The high-resolution image was taken at the location of 1 deg eccentricity from the center of the fovea with FOV1.5 (four images average).
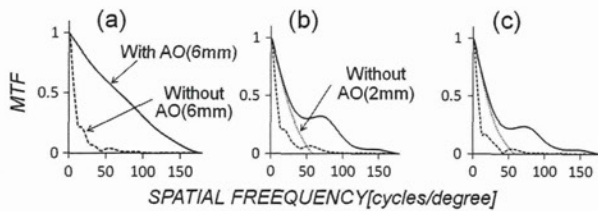
Fig. 5. MTFs. (a) FOV1.5; (b) FOV10 at the center of the fovea; (c) FOV10 at 5 deg nasal from the fovea.

that the AO function worked for normal eyes when focused at the photoreceptor layer of the retina to obtain FOV1.5 images, as in previous studies with catoptric and catadioptric systems [Fig. 3(c)]. We also successfully imaged the same areas of the retina with FOV3 and FOV10.

We performed imaging of the NFL with FOV10. The NFL could be imaged by moving the focus 68 μm toward the cornea by moving the focusing prism. The difference in focusing is shown in Fig. 4(a), and a montage NFL image is shown in Fig. 4(b). We experimentally confirmed that the same NFL imaging was not possible when the size of the beam for imaging was set to 2 mm.

We calculated modulation transfer functions (MTFs) for on-axis FOV1.5 imaging with and without AO. We also calculated MTFs for on and off-axis (5 deg) FOV10 over 6 mm pupil imaging with and without AO and over 2 mm pupil imaging without AO (Fig. 5). We found that the optics were almost perfect in FOV1.5 imaging with AO. However, the optics were not ideal in FOV10 imaging, even with AO. Although the MTF over a 2 mm pupil is better than that over a 6 mm pupil, as expected, the MTF over a 6 mm pupil with AO was better than that over a 2 mm pupil without AO for 50 to 80 cycles per degree.

FOV1.5 images and FOV10 images of the retina of an OMD patient with and without AO are shown in Fig. 6. The patient was a 51-year-old woman who visited Osaka University hospital with the complaint of decreased vision in both eyes. Her best corrected visual acuity was 20/100 in both eyes. The fundus picture was normal. However, multifocal electroretinography showed decreased responses in the macular areas of both eyes, which is typical in eyes with OMD. Fourier domain optical coherence tomography imaging has shown that the inner and outer segment (IS/OS) junction of the photoreceptors in the foveal area was disrupted, which was consistent with the previous report [9].

The FOV1.5 images of both small areas with AO were clearer than those without AO. The photoreceptors in the intact area were healthy, with a complete mosaic pattern.
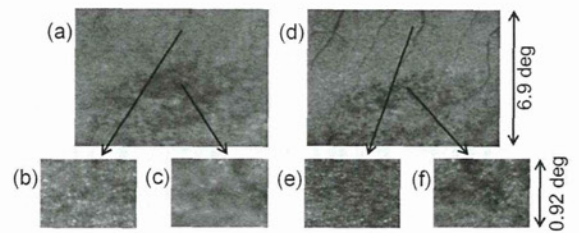

Fig. 6. Images of the photoreceptor layer of occult macular dystrophy. AO-OFF imaging (a) FOV10; (b) and (c) FOV1.5. AO-ON (d) FOV10; (e) and (f) FOV1.5. Images correspond to the arrows in the FOV10 images.

However, fewer photoreceptors were found in the diseased area. From these findings, we confirmed that the AO-DSO revealed the photoreceptor disruption in the eye with OMD with FOV1.5 images.

In the FOV10 images, the photoreceptors were not resolved, even with AO. Although we could not see the photoreceptors, the border of the normal and abnormal areas was much clearer in the image with AO than in that without AO. The AO-DSO allows for identification of the diseased area in the retina at a glance from the FOV10 images, reducing examination time.

AO-DSO was effective in the production of both FOV1.5 and FOV10 images. We were not troubled by noise from the refractive lenses during wavefront sensing and imaging. This demonstration that AO scanning ophthalmoscopes are useful for normal SLOs and very high-resolution imaging suggests that they may be useful in the clinical setting.

References

1. J. Liang, D. R. Williams, and D. T. Miller, J. Opt. Soc. Am. A **14**, 2884 (1997).
2. A. Roorda, F. Romero-Borja, W. Donnelly, III, H. Queener, T. Hebert, and M. Campbell, Opt. Express **10**, 405 (2002).
3. P. Godara, A. M. Dubis, A. Roorda, J. L. Duncan, and J. Carroll, Optometry Vision Sci. **87**, 930 (2010).
4. S. A. Burns, R. Tumbar, A. E. Elsner, D. Ferguson, and D. X. Hammer, J. Opt. Soc. Am. A **24**, 1313 (2007).
5. M. Mujat, R. D. Ferguson, A. H. Patel, N. Iftimia, N. Lue, and D. X. Hammer, Opt. Express **18**, 11607 (2010).
6. A. Dubra and Y. Sulai, Biomed. Opt. Express **2**, 1757 (2011).
7. M. Mujat, R. D. Ferguson, N. Iftimia, and D. X. Hammer, Opt. Express **17**, 10242 (2009).
8. Y. Zhang, S. Poonja, and A. Roorda, Opt. Lett. **31**, 1268 (2006).
9. Y. Kitaguchi, S. Kusaka, T. Yamaguchi, T. Mihashi, and T. Fujikado, Clin. Ophthalmol. **5**, 345 (2011).

Transcorneal Electrical Stimulation Promotes Survival of Photoreceptors and Improves Retinal Function in Rhodopsin P347L Transgenic Rabbits

Takeshi Morimoto,[1] *Hiroyuki Kanda,*[1] *Mineo Kondo,*[2] *Hiroko Terasaki,*[3] *Kohji Nishida,*[4] *and Takashi Fujikado*[1]

PURPOSE. To determine whether transcorneal electrical stimulation (TES) has neuroprotective effects on the photoreceptors, and whether it slows the rate of decrease of the electroretinogram (ERG) in rhodopsin P347L transgenic (Tg) rabbits.

METHODS. Six-week-old Tg rabbits received TES through a contact lens electrode on the left eye weekly for 6 weeks. The right eyes received sham stimulation on the same days. Electroretinograms (ERGs) were recorded before and at 12 weeks after the TES. After the last ERG recordings, the animals were euthanized for morphologic analysis of the retinas. Immunohistochemical (IHC) analysis was performed to detect the immunostaining by peanut agglutinin (PNA) and rhodopsin antibodies in the retinas.

RESULTS. The a- and b-wave amplitudes of the photopic ERGs and the b-wave amplitudes of the scotopic ERGs at higher stimulus intensities were significantly larger in the TES eyes than in the sham stimulated eyes ($P < 0.05$, respectively). Morphologic analyses showed that the mean thickness of the outer nuclear layer (ONL) in the visual streak at 12 weeks was significantly thicker in TES eyes than in sham-stimulated eyes ($P < 0.05$). IHC showed that the immunostaining by PNA and rhodopsin antibody in the TES-treated retinas was stronger than that in the sham-stimulated retinas.

CONCLUSIONS. TES promotes the survival of photoreceptors and preserves the ERGs in Tg rabbits. Although further investigations are necessary before using TES on patients, these findings indicate that TES should be considered for therapeutic treatment for RP patients with a P347L mutation of rhodopsin. (*Invest Ophthalmol Vis Sci.* 2012;53:4254–4261) DOI: 10.1167/iovs.11-9067

Patients with RP have a progressive loss of rod and cone photoreceptors that leads to a severe decrease in the visual acuity and a severe constriction of the visual field.[1,2] The worldwide prevalence of RP is approximately 1 in 4000, meaning that more than 1 million individuals are affected worldwide.[3] As such, RP is one of the leading causes of blindness in the world.

Many promising treatments to save or restore vision in RP patients are being investigated clinically and experimentally.[4–9] Electrical stimulation (ES) of the retina is one of the methods that is being tried because it is less invasive than other treatments and has been shown to have neuroprotective properties on the visual system.[10–18] ES of the transected optic nerve stump in rats promoted the survival of axotomized retinal ganglion cells (RGCs) in vivo.[10] Transcorneal electrical stimulation (TES) in rats was reported to rescue axotomized RGCs[11,12] and promote axonal regeneration of injured RGCs.[13,14] TES was also shown to improve the visual function of patients with traumatic optic neuropathy and nonarteritic ischemic optic neuropathy.[15]

We have demonstrated that TES promoted the survival of photoreceptors and preserved the retinal function of Royal College of Surgeons (RCS) rats, an animal model of RP.[16] Ni et al.[17] also reported that TES had neuroprotective effects on the photoreceptors after phototoxicity in rats. In a preliminary clinical trial, Schatz et al.[18] demonstrated that TES improved the visual function in RP patients.

However, RP is a genetically heterogeneous disease, and mutations in several photoreceptor-specific and some non-specific genes are known to cause RP.[19] Therefore, it is necessary to examine the neuroprotective effect of TES on the photoreceptors in the retinas of various RP animal models to determine which genetic type of RP is responsive to TES.

Rhodopsin Pro 347 Leu (P347L) transgenic (Tg) rabbits have been generated by Kondo et al.[20] This sequence of alterations is similar to those in human patients with autosomal dominant RP (adRP) with the rhodopsin P347L mutation.[21,22] This animal model has a rod-dominated, progressive photoreceptor degeneration with regional variations in the pattern of photoreceptor loss.[20,23]

The purpose of this study was to determine whether TES has a neuroprotective effect on the photoreceptors and improves the amplitudes of the electroretinogram (ERG) in Tg rabbits. Our morphologic and electrophysiological analyses showed that TES had a neuroprotective effect on the photoreceptors and improved the amplitudes of the ERG of Tg rabbits.

MATERIALS AND METHODS

Animals

All experimental procedures were performed in accordance with the ARVO Statement for the Use of Animals in Ophthalmic and Vision

Research, and the procedures were approved by the Animal Research Committee, Osaka University Graduate School of Medicine. Five Tg rabbits were purchased from the Kitayama Labes Co. (Ina, Japan). They were raised on a 12-hour dark 12-hour light cycle with an ambient light intensity of 100 lux.

Transcorneal Electrical Stimulation

The rabbits were anesthetized intramuscularly with a mixture of medetomidine (0.3 mg/kg, Domitor; Orion Corporation, Espoo, Finland), midazolam (4 mg/kg, Dormicum, Astellas Pharma Inc., Tokyo, Japan), and butorphanol (5 mg/kg, Betorphal; Meiji Seika Pharma, Co., Ltd., Tokyo, Japan). For the electrical stimulation, the corneas were also anesthetized with a drop of 0.4% oxybuprocaine HCl, and a contact lens electrode with inner and outer concentric electrodes (Mayo Corporation, Nagoya, Japan) was placed on the cornea with a drop of 2.5% methylcellulose to maintain good electrical contact and prevent corneal drying. Biphasic rectangular current pulses (700 μA, 10 ms/phase duration) were delivered at a frequency of 20 Hz from an electrical stimulation system (Stimulator: SEN-7320, Nihon Kohden, Tokyo, Japan; Isolator: WPI, Sarasota, FL) through the contact lens electrode.

TES was given to 6-week-old rabbits for 1 hour once a week until the animals were 12 weeks old. Only the left eye was electrically stimulated. The same type of contact lens electrode was placed on the right eyes but no electrical current was delivered (sham stimulation).

Electroretinograms

ERGs were recorded from the animals at 6 weeks of age just before the beginning of the TES and after the end of the TES treatments at 12 weeks of age. For the TES, animals were anesthetized intramuscularly with a mixture of medetomidine (0.3 mg/kg), midazolam (1 mg/kg), and butorphanol (1 mg/kg). The pupils were dilated with 2.5% phenylephrine hydrochloride and 0.5 % tropicamide.

After 1 hour of dark adaptation, the animals were restrained in a box and were prepared for the recordings under dim red light. ERGs were recorded from both eyes simultaneously with a corneal electrode carrying LEDs creating a mini-Ganzfeld stimulator (WLS-20, Mayo Corporation). A 2.5% hydroxypropyl methylcellulose ophthalmic solution was used with the corneal contact lens electrode. The reference electrode and a ground electrode were inserted subcutaneously into the left ear and the nose, respectively.

The luminance of the scotopic ERG stimuli was increased from −5.0 to 1.48 log cd·s/m² in 0.5 or 1.0 log unit steps. After the scotopic ERG recordings, animals were light-adapted for 30 minutes, and the photopic ERGs were recorded. The luminance of photopic ERG stimuli was increased from −1.0 to 1.95 log cd·s/m², and the stimuli were presented on a white background of 25 cd/m².

The responses were amplified, band pass filtered from 0.3 to 1000 Hz, and digitized at 3.3 kHz. A computational ERG recording system (Neuropack μ; Nihon Kohden, Tokyo, Japan) was used to average the ERG responses. Five to 20 responses were averaged with interstimulus intervals from 1 to 10 seconds depending on the intensity of the stimulus.

ERG Analysis

The scotopic (dark-adapted) and photopic (light-adapted) a-wave amplitudes were measured from the prestimulus baseline to the peak of the a-wave, and the b-wave amplitude was measured from the trough of the a-wave to the peak of b-wave.

To determine the significance of differences in the ERG amplitudes between TES electrically stimulated eyes and sham-stimulated eyes for the full intensity range, we plotted the average ratio of the TES-treated to the sham-stimulated eyes at all intensities and performed statistical analyses.[22-24]

Histological Analysis

Immediately after the final ERG recordings, the rabbits were euthanized with an overdose of pentobarbital sodium. The eyes were removed and placed in a mixture of 10% neutral buffered formalin and 2.5% glutaraldehyde in 0.1 M phosphate buffer (PB) for 30 minutes at room temperature. Then eyes were trimmed, and part of the eye cups, including the optic nerve, were postfixed in 4% glutaraldehyde in 0.1 M PB at 4°C. The tissues were trimmed, embedded in paraffin, sectioned vertically, and stained with hematoxylin and eosin for light microscopy. All sections were cut along the vertical meridian of the eye passing through the optic nerve. Five serial sections of each eye were analyzed for each experimental animal.

The degree of retinal degeneration was assessed by measuring the thickness of the outer nuclear layer (ONL), inner nuclear layer (INL), and ganglion cell layer (GCL). Photographs were taken of the superior and inferior hemispheres at 10 defined points with a camera attached to a light microscope (E800; Nikon, Tokyo, Japan). The first photograph was taken at approximately 2 mm from the center of the optic nerve head, and subsequent photographs were taken every 2 mm more peripherally. The thickness of ONL, INL, and GCL were measured on the photographs (Scion Image analyzer; Scion Corp., Frederick, MD). Each eye was coded so that the investigator making the measurements was masked to treatment of the eye.

Immunohistochemistry

The paraffin-embedded sections (5 μm) were processed for immunofluorescence staining with antirhodopsin antibody (1:100; RET-P1; Santa Cruz Biotechnology, Santa Cruz, CA), followed by Cy3-conjugated anti-mouse IgG (1:200), and FITC-conjugated peanut agglutinin (1:100) (PNA; Invitrogen, Carlsbad, CA), a lectin that binds specifically to rabbit cone photoreceptors. The TES-treated and sham-stimulated sections were observed with a fluorescence microscope (E800; Nikon).

Statistical Analysis

Data were analyzed with a commercial software (JMP8; SAS Institute Japan, Tokyo, Japan). The data were expressed as the means ± SDs or SEMs. Comparisons between two groups were made by Student's t-tests when the data were normally distributed or by the Mann-Whitney rank-sum test when the data were not normally distributed. Statistical significance was set at $P < 0.05$.

RESULTS

Effect of TES on Survival of Photoreceptors in Tg Rabbits

Representative retinal sections in the area of the visual streak from 12-week-old Tg rabbits that had TES (left eye) or sham stimulation (right eye) are shown in Figures 1A and 1B. The number of rows of nuclei in the ONL at the visual streak was two to three and the nuclei were closely packed in the retina receiving TES (Fig. 1A). In the sham-stimulated retina, only one row of nuclei was found in the ONL at the visual streak and they were loosely packed (Fig. 1B). In contrast, there was no difference in the structure and thickness of the ONL in other areas of the retina away from the visual streak between the TES-treated and sham-stimulated retinas (Figs. 1C, 1D). The architecture and thickness of the middle and inner retinal layers were well preserved in both TES-treated and sham-stimulated retinas (Figs. 1A–D).

Quantitative analyses showed that the thickness of the ONL in the visual streak in the TES-treated eyes was 13.9 ± 3.3 μm
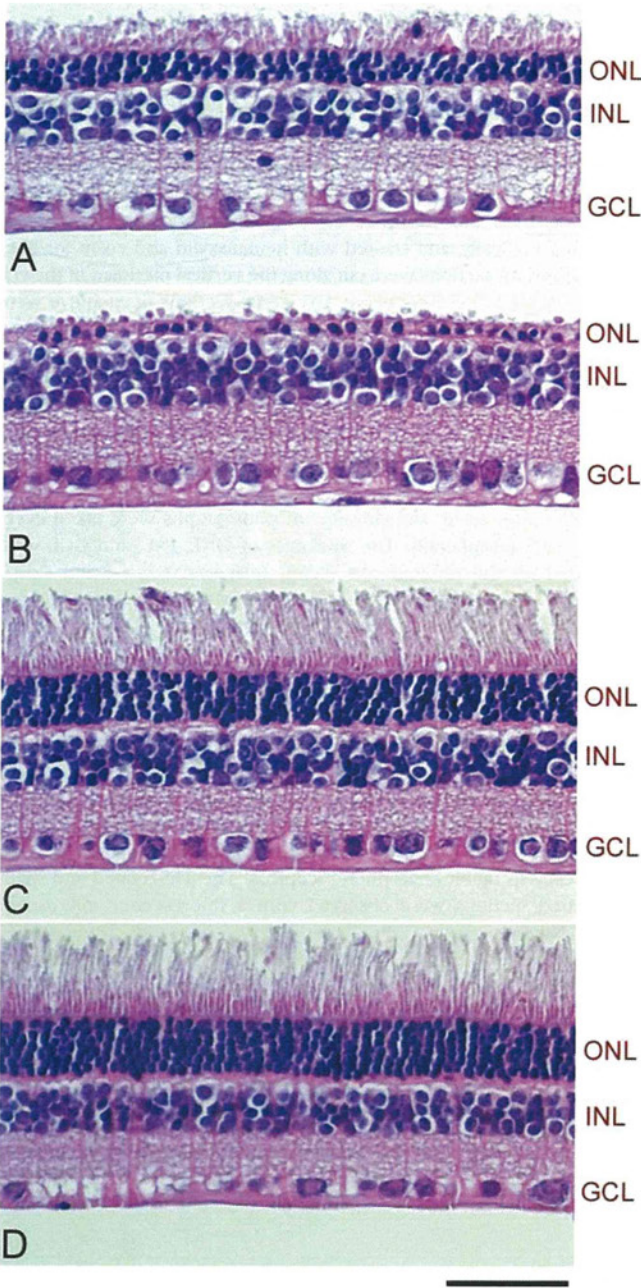
FIGURE 1. Photomicrographs of TES-treated and sham-stimulated retinas from 12-week-old Tg rabbits. Retinal sections of the visual streak from TES-treated retina (**A**) and sham-stimulated retina (**B**). Peripheral retinas at 6 mm superior to the optic nerve head from TES-treated retina (**C**) and sham-stimulated retina (**D**). Scale bar = 50 μm.

(mean ± SD, $n = 5$) which was significantly thicker than that in the sham-stimulated eyes (8.8 ± 2.8 μm, $n = 5$, $P < 0.05$) (inferior hemisphere 1). In contrast, there was no significant difference in the mean ONL thickness outside the area of the visual streak (Fig. 2A). Thus, TES promoted the survival of photoreceptors in the area of the visual streak at 12 weeks of age.

To determine whether TES affected other layers of the retina, we measured the thickness of the INL and GCL. There were no significant differences of the mean thickness of INL and GCL between the TES retinas and in the sham retinas ($n = 5$ each; Figs. 2B, 2C).

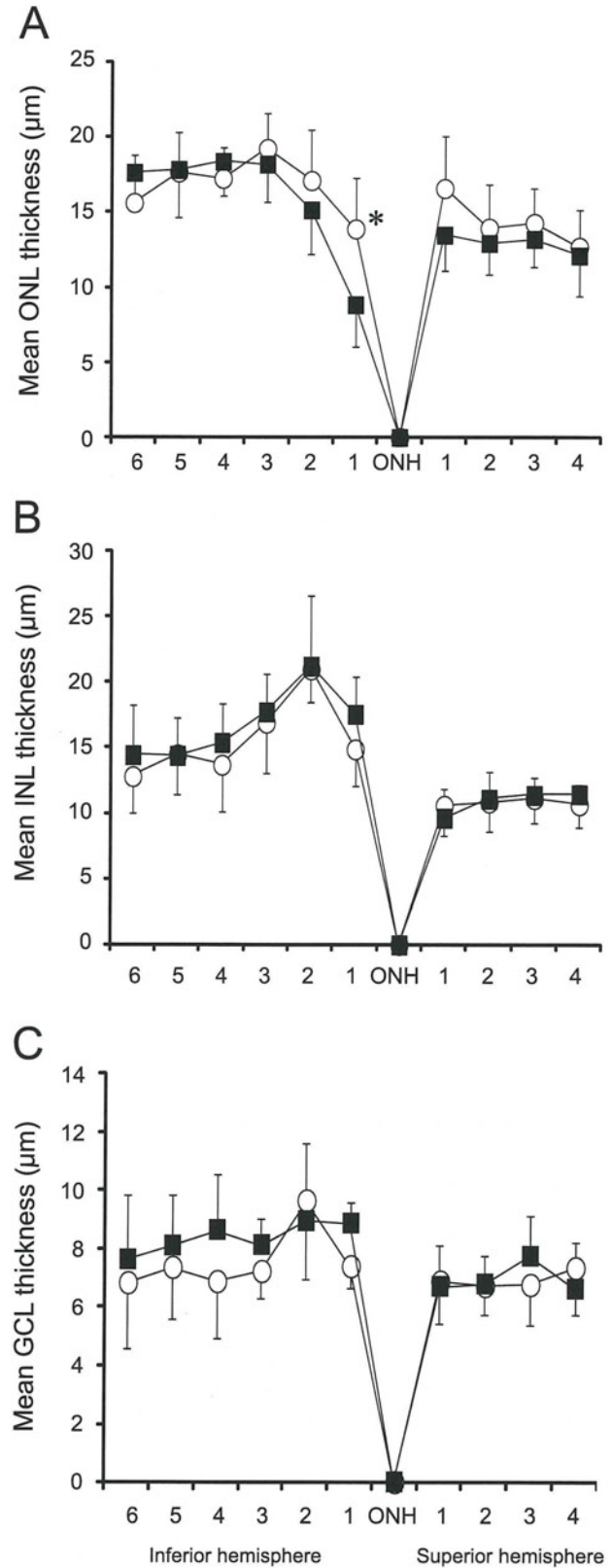**FIGURE 2.** Thickness of the ONL (**A**), the INL (**B**), and the GCL (**C**) along the vertical meridian measured at 10 retinal locations at 2-mm intervals. Mean ± SD of five Tg rabbits are plotted. There was a significant difference of the mean ONL thickness between TES-treated retinas (○) and sham-stimulated retina (■) at the visual streak (Student's *t*-test for two groups; *$P < 0.05$).

FIGURE 3. Scotopic ERGs recorded from 6- and 12-week-old rhodopsin P347L Tg rabbits. (A) Scotopic ERGs elicited by eight different stimulus intensities. (B) Scotopic ERG mean amplitude versus flash intensity for the a- and b-waves in the TES-treated (○) and sham-stimulated eyes (■) (n = 5, each, mean ± SEM). Average ratio (TES/sham) of the a- (C) and b-wave (D) amplitudes at 12 weeks of age (n = 5, each, mean ± SEM). Pointwise comparison indicated a significant difference in b-wave amplitudes at 1.48 and 0.95 log cd·s/m² (Student's t-tests for two groups; *P < 0.05).
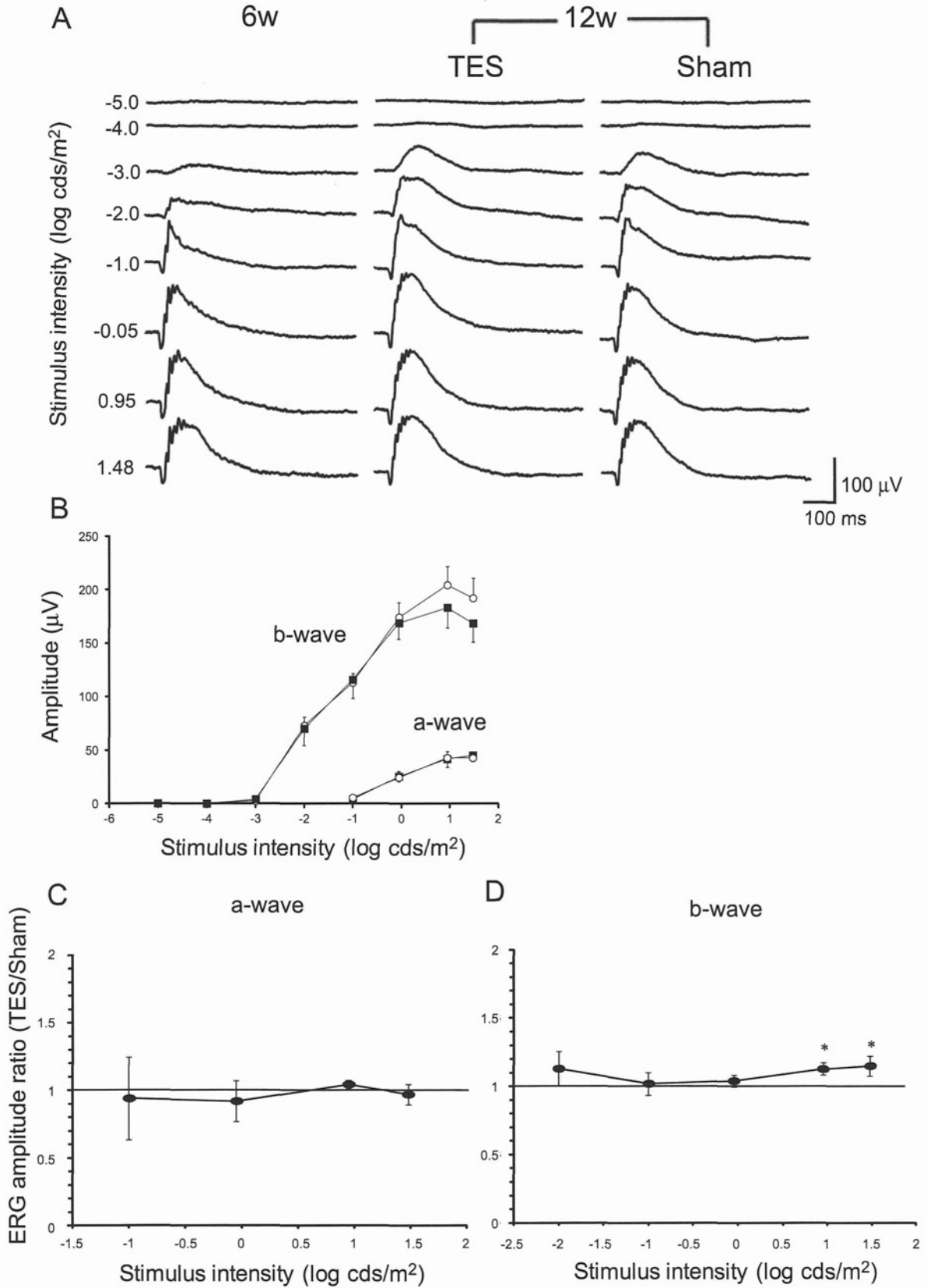
FIGURE 4.   Photopic ERGs recorded from 6- and 12-week-old rhodopsin P347L Tg rabbits. (**A**) Photopic ERGs elicited by five different stimulus intensities. (**B**) Photopic ERG mean amplitude versus flash intensity for the a- and b-waves in the TES-treated (○) and sham-stimulated (■) retinas. Average ratio (TES/sham) of the a- (**C**) and b-wave (**D**) amplitudes at 12 weeks of age ($n = 5$, each, mean ± SEM). Pointwise comparison indicated a significant difference in a-wave amplitudes at 0.95 to 1.95 log cd·s/m² (Student's *t*-tests for two groups; *$P < 0.05$, **$P < 0.01$), and in b-wave amplitudes at 1.48 and 1.95 log cd·s/m² (Student's *t*-tests for two groups; *$P < 0.05$, **$P < 0.01$).

Effect of TES on Electroretinograms of Tg Rabbits

To evaluate the electrical properties of the rod and cone systems of rabbits, we recorded full-field scotopic and photopic ERGs. The scotopic ERGs elicited by different stimulus intensities from 6- and 12-week-old Tg rabbits are shown in Figure 3A. The amplitudes of the scotopic ERGs recorded from the eyes of 12-week-old Tg rabbits were not reduced compared with those from the eyes of 6-week-old Tg rabbits. The intensity–response curves for the a- and b-waves are plotted in Figure 3B. Scotopic ERG a-wave amplitudes of TES-treated eyes were not significantly different from those of sham-stimulated eyes. However, the b-wave amplitudes of the TES-treated eyes were slightly but significantly larger than those of the sham-stimulated eyes at the higher stimulus intensities.

We plotted the ratio (TES/sham-stimulated eye) of the amplitudes of the a- and b-waves for all intensities and performed statistical analyses on the differences (Figs. 3C, 3D). The differences in the ratios of the a-waves were not significant for all intensities. On the other hand, the ratios of the b-wave amplitudes were significantly larger at stimulus intensities higher than 0.95 log cd·s/m^2 ($P < 0.05$) in the TES-treated eyes.

The photopic ERGs obtained from Tg rabbits at 6 and 12 weeks of age are also shown in Figure 4A. The amplitudes of the TES-treated and sham-stimulated eyes at 12 weeks of age were slightly reduced compared with the ERGs recorded from 6-week-old Tg rabbits but the differences were not significant. However, the responses in the eye treated with TES were larger than those treated with sham stimulation (Fig. 4A).

The intensity–response curve for the a- and b-waves are plotted in Figure 4B. We also plotted the average ratio of TES-treated to sham-stimulated eyes at all intensities (Figs. 4C, 4D). For a-waves, there were significant differences between TES-treated and sham-stimulated eyes at 0.95 to 1.95 log cd·s/m^2 ($P < 0.05$, respectively). For b-waves, there were significant differences between them at 1.48 and 1.95 log cds/m^2 ($P < 0.05$).

Immunohistochemistry

Immunostaining with an antirhodopsin antibody and PNA lectin showed that the intensities of the immunostaining for both antirhodopsin antibody and PNA were stronger in the TES-treated retina (Figs. 5A–C) than the sham-stimulated retina (Figs. 5D–F).

Discussion

Our electrophysiological and histological analyses showed that TES led to the survival of photoreceptors in the visual streak, and it also led to the preservation of ERG responses at higher stimulus intensities in rhodopsin P347L Tg rabbits. Although the cause of the photoreceptor degeneration in Tg rabbits is different from that in RCS rats and the phototoxic-induced degeneration in rats,[20,23,25–27] TES also had a neuroprotective effect on the photoreceptors in Tg rabbits. These findings indicate that TES might have a similar neuroprotective effect on photoreceptors whose degeneration has different causes.

In the histological analysis, only the photoreceptors in the visual streak were rescued by TES, and in the areas outside the visual streak, the number of photoreceptors in the TES-treated retina was not significantly different from that in sham-stimulated retina. In Tg rabbits, the loss of photoreceptors was maximum in the visual streak where the photoreceptor density is highest, and the loss of photoreceptors was not significantly different at other regions outside visual streak at 12 weeks of age.[20] Therefore, at 12 weeks of age, the loss of photoreceptors was striking only in the visual streak, indicating that the neuroprotection of photoreceptors was limited to the visual streak.

Immunohistochemical analysis showed that the intensity of both PNA and rhodopsin immunostainings was stronger in the TES-treated retinas than in the sham-stimulated retinas in the visual streak.

However, the results of ERGs indicated that TES preserved the cone components better than rod components, although in Tg rabbits the rod components are more affected than the cones.[20,23] Although it was not determined why the cone components were better preserved than the rod components, one possibility is that TES promoted the survival of both rod and cone photoreceptors, and the rescued rods secreted a cone viability factor to rescue the cone photoreceptors.[28] Otherwise, at 12 weeks of age, photoreceptors near the visual streak were much more affected than those outside the visual streak,[20] therefore the differences of ERG amplitudes of full field ERGs between TES-treated and sham-stimulated retinas might be detected only at higher stimulus intensities.

There are some possible mechanisms for the neuroprotection of photoreceptors. First, TES increased the expression of the mRNA and protein levels of neurotrophic factors (e.g., insulin-like growth factor-1 (IGF-1), brain-derived neurotrophic
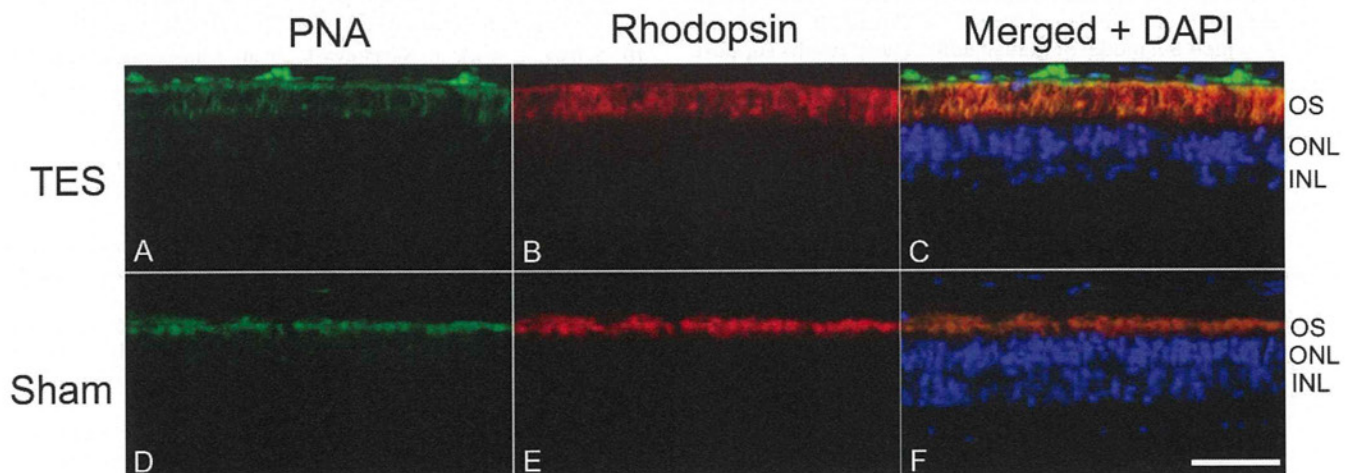

PNA   Rhodopsin   Merged + DAPI

Figure 5. Immunohistochemical analysis of rod and cone photoreceptors triple labeled with rhodopsin (*green*), PNA (*red*), and DAPI (*blue*) in TES-treated (A–C) and sham-stimulated retinas (D–E) at 12 weeks of age (approximately 4 mm inferior to the optic nerve head). Intensities of rhodopsin and PNA immunostaining are stronger in the TES-treated ratio than in the sham-stimulated retina. Scale bar = 50 μm.

factor (BDNF), ciliary neurotrophic factor, or B-cell lymphoma-2 in the retinas after TES.[11,17] A second possibility is that TES reduced the expression of the TNF super families and Bax, which are related to apoptosis signaling in retinal cells.[29] Cultured rat Müller cells exposed to electrical currents have been shown to express IGF-1, BDNF, and fibroblast growth factor-2 (FGF-2).[30-32] Other types of electrical stimulation to the retinas, such as subretinal electrical stimulation, increases the expression of FGF-2 in the retinas.[33] Unfortunately, we did not determine whether the expression of any of these neurotrophic factors was increased after TES in the Tg rabbit retinas.

Another possible mechanism for the TES-induced neuroprotection was an increase of chorioretinal blood circulation by TES.[34,35] In clinical studies, TES has been shown to improve the visual function of patients with retinal artery occulsion.[36,37] Thinning of the vascular plexus and the development of aberrant vessels have been reported in RP patients and animal models of RP.[38-41] This indicates that retinal blood circulation might be reduced in Tg rabbits. TES might have some neuroprotective effects on photoreceptors by increasing chorioretinal blood circulation.

We did not examine whether TES was neuroprotective for the photoreceptors in the peripheral retina. In Tg rabbits at the age of 48 weeks, almost all of the photoreceptors were lost[20,27]; however, it takes a long time to investigate the neuroprotective effects of TES on the entire retina until the age of 48 weeks from 6 weeks, so it is difficult to continue the treatment until 48 weeks because weekly anesthesia and treatment put a heavy load on animals and is adverse to the animal welfare for long-term experiments. The results that TES did have neuroprotective effects on photoreceptors in the visual streak at 12 weeks of age were enough to lead us to determine the neuroprotection of TES on the photoreceptors in Tg rabbits.

Rhodopsin P347L Tg rabbits are an adRP model of human RP. Our results indicate that TES might have a neuroprotective effect on the photoreceptors in RP patients with the same mutation. Schatz et al.[18] performed a prospective, randomized sham-controlled clinical study, and reported that TES improved the visual function in RP patients. From these neuroprotective effects of TES already published and our results, TES might exert a neuroprotective effect on photoreceptors of different animals with RP. Additional investigations on different animal models are necessary to determine which type of RP was the indication of TES treatment.

In conclusion, TES had a neuroprotective effect on the photoreceptors in the visual streak of rhodopsin P347L Tg rabbits, which is a model of human adRP. These results support and encourage clinical trials of TES for RP patients.

References

1. Marmor MF, Aguirre G, Arden G, et al. Retinitis pigmentosa: a symposium on terminology and methods of examination. *Ophthalmology.* 1983;90:126–131.

2. Pagon RA. Retinitis pigmentosa. *Surv Ophthalmol.* 1988;33:137–177.

3. Hartong DT, Berson EL, Dryja TP. Retinitis pigmentosa. *Lancet.* 2006;368:1795–1809.

4. Berson EL, Rosner B, Sandberg MA, et al. A randomized trial of vitamin A and vitamin E supplementation for retinitis pigmentosa. *Arch Ophthalmol.* 1993;111:761–772.

5. Sieving PA, Caruso RC, Tao W, et al. Ciliary neurotrophic factor (CNTF) for human retinal degeneration: phase I trial of CNTF delivered by encapsulated cell intraocular implants. *Proc Natl Acad Sci U S A.* 2006;103:3896–3901.

6. Ali RR, Sarra GM, Stephens C, et al. Restoration of photoreceptor ultrastructure and function in retinal degeneration slow mice by gene therapy. *Nat Genet.* 2000;25:306–310.

7. Bainbridge JW, Smith AJ, Barker SS, et al. Effect of gene therapy on visual function in Leber's congenital amaurosis. *N Engl J Med.* 2008;358:2231–2239.

8. Zrenner E, Bartz-Schmidt KU, Benav H, et al. Subretinal electronic chips allow blind patients to read letters and combine them to words. *Proc Biol Sci.* 2011;278:1489–1497.

9. Fujikado T, Kamei M, Sakaguchi H, et al. Testing of semi-chronically implanted retinal prosthesis by suprachoroidal-transretinal stimulation in patients with retinitis pigmentosa. *Invest Ophthalmol Vis Sci.* 2011;52:4726–4733.

10. Morimoto T, Miyoshi T, Fujikado T, Tano Y, Fukuda Y. Electrical stimulation enhances the survival of axotomized retinal ganglion cells in vivo. *NeuroReport.* 2002;13:227–230.

11. Morimoto T, Miyoshi T, Matsuda S, Tano Y, Fujikado T, Fukuda Y. Transcorneal electrical stimulation rescues axotomized retinal ganglion cells by activating endogenous retinal IGF-1 system. *Invest Ophthalmol Vis Sci.* 2005;46:2147–2155.

12. Morimoto T, Miyoshi T, Sawai H, Fujikado T. Optimal parameters of transcorneal electrical stimulation (TES) to be neuroprotective of axotomized RGCs in adult rats. *Exp Eye Res.* 2010;90:285–291.

13. Miyake K, Yoshida M, Inoue Y, Hata Y. Neuroprotective effect of transcorneal electrical stimulation on the acute phase of optic nerve injury. *Invest Ophthalmol Vis Sci.* 2007;48:2356–2361.

14. Tagami Y, Kurimoto T, Miyoshi T, Morimoto T, Sawai H, Mimura O. Axonal regeneration induced by repetitive electrical stimulation of crushed optic nerve in adult rats. *Jpn J Ophthalmol.* 2009;53:257–266.

15. Fujikado T, Morimoto T, Matsushita K, Shimojo H, Okawa Y, Tano Y. Effect of transcorneal electrical stimulation in patients with nonarteritic ischemic optic neuropathy or traumatic optic neuropathy. *Jpn J Ophthalmol.* 2006;50:266–273.

16. Morimoto T, Fujikado T, Choi JS, et al. Transcorneal electrical stimulation promotes the survival of photoreceptors and preserves retinal function in royal college of surgeons rats. *Invest Ophthalmol Vis Sci.* 2007;48:4725–4732.

17. Ni YQ, Gan DK, Xu HD, Xu GZ, Da CD. Neuroprotective effect of transcorneal electrical stimulation on light-induced photoreceptor degeneration. *Exp Neurol.* 2009;219:439–452.

18. Schatz A, Röck T, Naycheva L, et al. Transcorneal electrical stimulation for patients with retinitis pigmentosa: a prospective, randomized, sham-controlled exploratory study. *Invest Ophthalmol Vis Sci.* 2011;23:4485–4496.

19. Daiger SP, Bowne SJ, Sullivan LS. Perspective on genes and mutations causing retinitis pigmentosa. *Arch Ophthalmol.* 2007;125:151–158.

20. Kondo M, Sakai T, Komeima K, et al. Generation of a transgenic rabbit model of retinal degeneration. *Invest Ophthalmol Vis Sci.* 2009;50:1371–1377.

21. Oh KT, Longmuir R, Oh DM, et al. Comparison of the clinical expression of retinitis pigmentosa associated with rhodopsin mutations at codon 347 and codon 23. *Am J Ophthalmol.* 2003;136:306–313.

22. Berson EL, Rosner B, Sandberg MA, et al. Ocular findings in patients with autosomal dominant retinitis pigmentosa and rhodopsin, proline-347-leucine. *Am J Ophthalmol.* 1991;111:614–623.

23. Sakai T, Kondo M, Ueno S, et al. Supernormal ERG oscillatory potentials in transgenic rabbit with rhodopsin P347L mutation

and retinal degeneration. *Invest Ophthalmol Vis Sci.* 2009;50: 4402–4409.

24. Bush RA, Lei B, Tao W, et al. Encapsulated cell-based intraocular delivery of ciliary neurotrophic factor in normal rabbit: dose-dependent effects on ERG and retinal histology. *Invest Ophthalmol Vis Sci.* 2004;45:2420–2430.

25. D'Cruz PM, Yasumura D, Weir J, et al. Mutation of the receptor tyrosine kinase gene Mertk in the retinal dystrophic RCS rat. *Hum Mol Genet.* 2000;9:645–651.

26. Noell WK, Walker VS, Kang BS, Berman S. Retinal damage by light in rats. *Invest Ophthalmol.* 1966;5:450–473.

27. Jones BW, Kondo M, Terasaki H, et al. Retinal remodeling in the Tg P347L rabbit, a large-eye model of retinal degeneration. *J Comp Neurol.* 2011;519:2713–2733.

28. Léveillard T, Mohand-Saïd S, Lorentz O, et al. Identification and characterization of rod-derived cone viability factor. *Nat Genet.* 2004;36:755–759.

29. Willmann G, Schäferhoff K, Fischer MD, et al. Gene expression profiling of the retina after transcorneal electrical stimulation in wildtype brown Norway rats. *Invest Ophthalmol Vis Sci.* 2011;52:7529–7537.

30. Sato T, Lee TS, Takamatsu F, Fujikado T. Induction of fibroblast growth factor-2 by electrical stimulation in cultured retinal Mueller cells. *Neuroreport.* 2008;19:1617–1621.

31. Sato T, Fujikado T, Morimoto T, Matsushita K, Harada T, Tano Y. Effect of electrical stimulation on IGF-1 transcription by L-type calcium channels in cultured retinal Müller cells. *Jpn J Ophthalmol.* 2008;52:217–223.

32. Sato T, Fujikado T, Lee TS, Tano Y. Direct effect of electrical stimulation on induction of brain-derived neurotrophic factor

33. Ciavatta VT, Kim M, Wong P, et al. Retinal expression of Fgf2 in RCS rats with subretinal microphotodiode array. *Invest Ophthalmol Vis Sci.* 2009;50:4523–4530.

34. Kurimoto T, Oono S, Oku H, et al. Transcorneal electrical stimulation increases chorioretinal blood flow in normal human subjects. *Clin Ophthalmol.* 2010;4:1441–1446.

35. Mihashi T, Okawa Y, Miyoshi T, Kitaguchi Y, Hirohara Y, Fujikado T. Comparing retinal reflectance changes elicited by transcorneal electrical retinal stimulation with those of optic chiasma stimulation in cats. *Jpn J Ophthalmol.* 2011;55:49–56.

36. Inomata K, Shinoda K, Ohde H, et al. Transcorneal electrical stimulation of retina to treat longstanding retinal artery occlusion. *Graefes Arch Clin Exp Ophthalmol.* 2007;245: 1773–1780.

37. Oono S, Kurimoto T, Kashimoto R, Tagami Y, Okamoto N, Mimura O. Transcorneal electrical stimulation improves visual function in eyes with branch retinal artery occlusion. *Clin Ophthalmol.* 2011;5:397–402.

38. Spalton DJ, Bird AC, Cleary PE. Retinitis pigmentosa and retinal oedema. *Br J Ophthalmol.* 1978;62:174–182.

39. Uliss AE, Gregor ZJ, Bird AC. Retinitis pigmentosa and retinal neovascularization. *Ophthalmology.* 1986;93:1599–1602.

40. Matthes MT, Bok D. Blood vascular abnormalities in the degenerative mouse retina (C57BL/6J-rd le). *Invest Ophthalmol Vis Sci.* 1984;25:364–369.

41. Wang S, Villegas-Pérez MP, Vidal-Sanz M, Lund RD. Progressive optic axon dystrophy and vacuslar changes in rd mice. *Invest Ophthalmol Vis Sci.* 2000;41:537–545.

from cultured retinal Müller cells. *Invest Ophthalmol Vis Sci.* 2008;49:4641–4646.

Clinical Trial of Chronic Implantation
of Suprachoroidal-Transretinal Stimulation System
for Retinal Prosthesis

Takashi Fujikado*, Motohiro Kamei[1], Hirokazu Sakaguchi[1],
Hiroyuki Kanda, Takeshi Morimoto, Yasushi Ikuno[1], Kentaro Nishida[1],
Haruhiko Kishima[2], Tomoyuki Maruo[2], Hajime Sawai[3],
Tomomitsu Miyoshi[3], Koji Osawa[4] and Motoki Ozawa[4]

Department of Applied Visual Science, Osaka University Graduate School of Medicine,
2-2 Yamadaoka, Suita, Osaka 565-0871, Japan
[1]Department of Ophthalmology, Osaka University Graduate School of Medicine,
2-2 Yamadaoka, Suita, Osaka 565-0871, Japan
[2]Department of Neurosurgery, Osaka University Graduate School of Medicine,
2-2 Yamadaoka, Suita, Osaka 565-0871, Japan
[3]Department of Integrative Physiology, Osaka University Graduate School of Medicine,
2-2 Yamadaoka, Suita, Osaka 565-0871, Japan
[4]Nidek Co., 34-14 Maehama, Hiroishi, Gamagori, Aichi 443-0038, Japan

Retinal prosthesis is an implantable medical device to reconstruct the sense of sight for blind individuals. We have been developing a new type of retinal prosthesis called suprachoroidal-transretinal stimulation (STS), whereby an electrode array is not attached to the retina directly. To evaluate the feasibility and safety of the retinal prosthesis using STS, a clinical trial was performed. We have developed an internal device for chronic implantation. It consists of a 49-channel electrode array that has 9 active electrodes. The retinal prosthesis was implanted in two patients with advanced retinitis pigmentosa (RP). Follow-up periods after implantation were five (Pt 1) and seven (Pt 2) weeks. No significant adverse event was observed in either patient after the surgical procedures. A functional test revealed that the detection or discrimination of objects was possible using the device, and a pulse frequency of around 20 Hz is the most effective in evoking phosphene. These clinical examinations showed that the retinal prosthesis with the STS system is safe and feasible for artificial vision.

---

*Corresponding author: e-mail: fujikado@ophthal.med.osaka-u.ac.jp

1. Introduction

Retinitis pigmentosa (RP) is one of the leading causes of blindness.[1] There is no treatment for this disease. To restore some vision, stimulating the residual functional retinal neurons by electrical currents delivered through an electrode array is being studied. This is called "retinal prosthesis".

There are three ways of stimulating the retina for a retinal prosthesis: subretinal stimulation,[2] epiretinal stimulation,[3] and suprachoroidal-transretinal stimulation (STS).[4–6] In subretinal stimulation, the electrode array is placed in the subretinal space. In epiretinal stimulation, the electrode array is attached to the vitreous side of the retina. In STS, the electrode array is placed in a scleral pocket or choroidal membrane and the return electrode in the vitreous cavity. STS was originally designed by our group. The main feature of STS is that the electrode array is not directly attached to the retina. Therefore, it can minimize damage to the retina during the electrode implantation surgery.

For clinical application of the retinal prosthesis with STS, it is important to evaluate its feasibility and safety through clinical trial. For that reason, we have developed a microelectrode-STS system that can be chronically implanted into the patient. The purpose of this study is to evaluate the safety and stability of the system when it is implanted in a patient with RP.

2. Materials and Methods

2.1 Subjects

Two patients with RP were studied. Patient 1 (Pt 1) was a 73-year-old woman. Patient 2 (Pt 2) was a 67-year-old woman. Visual acuity of both patients was light perception. We obtained informed consent from these patients after a full explanation of the purpose of the study and the procedures. The procedures used in this study adhered to the Declaration of Helsinki and were approved by the Ethics Committee of Osaka University Hospital.

2.2 Retinal prosthesis devices for implantation

The implanted electronic devices consisted of a secondary coil that receives signals from the external coil and a pulse generator that generates biphasic current pulses to be delivered to the individual electrodes sequentially. The electrode array (size, 5.7×4.6 mm²; NIDEK, Gamagori, Japan) consisted of 49 electrodes made of 0.5-mm-diameter platinum (Fig. 1).

2.3 Surgery

In both patients, the left eye was selected for the clinical trial. Under local anesthesia with 2% lidocaine hydrochloride drops, the lateral rectus muscle was dissected at its insertion, and transscleral monopolar stimuli were given to determine the scleral area that has a low threshold to evoke phosphene perception. After the identification and marking of the low-threshold area, general anesthesia was introduced. The skin of the
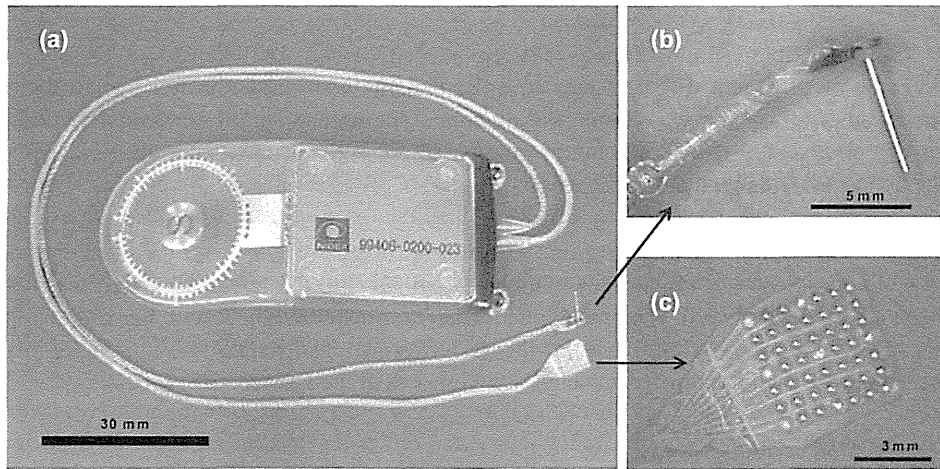
Fig. 1. Photographs of the internal device for STS-retinal prosthesis (a), the electrode array (b), and the return electrode (c).

left temporal area was incised to insert the main part of the internal device [Fig. 1(a)]. The second incision was created at the left zygomatic bone area to fix the lead wire. The electrode array, the return electrode, and the cables were passed under the fascia of the temporal muscle from the first incision to the second incision using a trocar catheter (Medikit, Tokyo, Japan). The bone of the lateral orbital wall was drilled, and the electrode array, the return electrode, and the lead wire were passed into the periocular space using the trocar catheter. The lead wire was fixed by a titanium plate below the second incision. A scleral pocket of 6×5 mm^2 was created at the lower temporal scleral area at the low-threshold area. The electrode array was inserted into the scleral pocket. The return electrode was inserted in the vitreous cavity through the pars plana at the upper nasal area. The lead wires near these electrodes were sutured on the sclera. Five (Pt 1) to seven (Pt 2) weeks after the implantation, all the devices were surgically removed.

2.4　*Functional tests*

From one week after the surgery, the wireless system was tested twice a week for 4 weeks. For the functional test of each electrode, 9 out of the 49 electrodes were tested. Cathodic-first biphasic pulses (pulse duration, 0.5 ms; frequency, 20 Hz; interpulse delay, 0.5 ms) were delivered through each electrode. We performed the following six visual function tests.

2.4.1　*Test 1: Object detection*

A white box that was 2.6×27 cm (3.7×34° visual angle) was set randomly at 15 cm (21°) to the left or right of the center of the board. The patients were asked where the white box was located. The percentage of correct answers for this task was analyzed statically by the binominal test. We tested whether the percentage was higher than the chance level (50%).

2.4.2 *Test 2: Object discrimination*

Two bars of different widths, 1×30 cm (1.4×37°) and 3×30 cm (4.3×3.7°), were presented at the center of the board, and the patients were asked to tell the examiner whether the thicker bar was on the left or right. The percentage of correct answers for this task was analyzed statically by the binominal test. We tested whether the percentage was higher than the chance level (50%).

2.4.3 *Test 3: Grasping objects*

A white object was randomly set either 15 cm (21°) to the left or 15 cm to the right of the center of the board. The patient was asked to grasp the object with her right hand. The percentage of correct answers for this task was analyzed statically by the binominal test. We tested whether the percentage was higher than the chance level (50%).

2.4.4 *Test 4: Touch panel*

A white rectangular bar of 4.7×20 cm (6.7×27°) was presented randomly 9.5 cm (13°) to the left or the right from the center of a touch panel screen (Tyco Electronics, Menlo Park, CA) that was connected to a computer. The patient was asked to touch the white bar with her right index finger. The position touched was recorded and analyzed using the computer. Depending on whether the patient touched the correct position, a different sound was emitted by the computer.

2.4.5 *Test 5: Relationship between pulse frequency and brightness of phosphenes*

We examined the relationship between the brightness of phosphenes and pulse frequency using suprathreshold currents (0.8 mA) in Pt 2. The pulse train duration was 1 s. We selected two out of the following frequencies: 10, 20, and 50 Hz. We applied these stimulations to the patient randomly. The patient was asked to compare the brightness of phosphenes evoked by two types of stimulation with different frequencies. Each trial was repeated 4 times.

3.   Results and Discussion

After the surgery, it was confirmed that the device, cables, and electrodes were implanted and connected, on the basis of skull X-ray projections (Fig. 2). From the fundus picture, fluorescein angiograms, and optical coherence tomography (OCT) images, no significant adverse event was attributed to the implantation surgery in both patients. After the removal surgery, no significant changes were observed in the fundus picture and OCT images. The visual acuity remained at light perception after the removal of the device in both patients. At the removal surgery, the scleral pocket remained stable. Fibrosis or erosion of sclera was not observed around the pocket. The implanted devices and electrode array were kept functional during the 4 weeks of examination and after the removal of the device. Moreover, corrosion was not observed on the surface of electrodes. These results indicated the safety of our STS approach for a retinal prosthesis and also the durability of the implantable device.
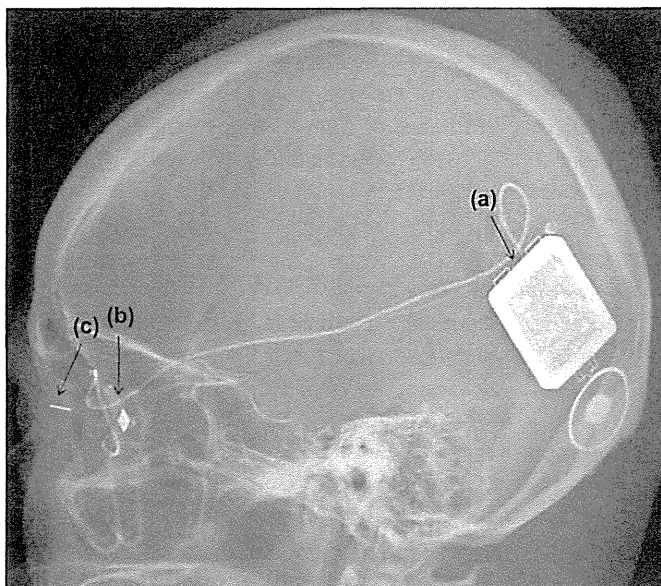
Fig. 2.   Lateral view of skull XP of Pt 1. (a) Internal device that has pulse generator circuit and decoder circuit. (b) Electrode array. (c) Return electrode.

Both patients scored better than chance in the object detection and object discrimination tasks with head scanning (Fig. 3). The grasping objects task was carried out by Pt 2 because the elicited phosphene was located close to the subjective center. The score (90%) was significantly better than chance. The touch panel task was also applied to only Pt 2. The success rate increased when the testing was repeated (Fig. 4). These functional tests revealed that object discrimination was possible even with a small number of active electrodes.

The subjective phosphenes tended to be brighter at a frequency of 20 Hz than that at 10 or 50 Hz (Fig. 5). This test was applied to only Pt 2. This result is consistent with the results of transscleral electrical stimulation.[7] These results suggest that a frequency of around 20 Hz is the most effective to stimulate the retina of not only a healthy subject but also an RP patient.

4.   Conclusions

We implanted a retinal prosthesis in two patients with advanced RP. No significant adverse event was observed in either patient after the surgical procedures, confirming the safety of our surgical methods. Functional testing revealed that the detection and discrimination of objects were possible by head scanning with a small number of active
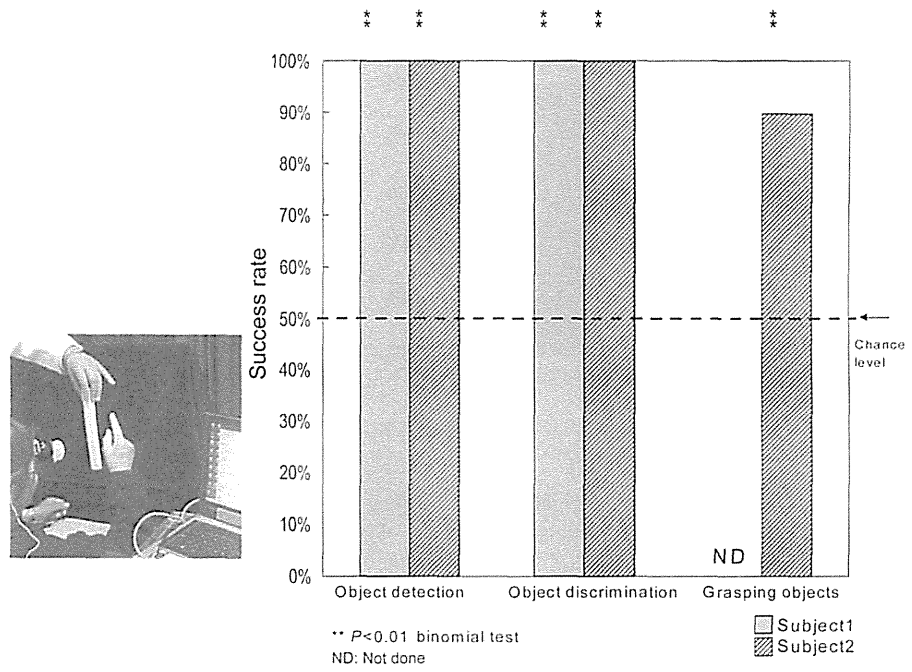
Fig. 3. Success rate of functional test.
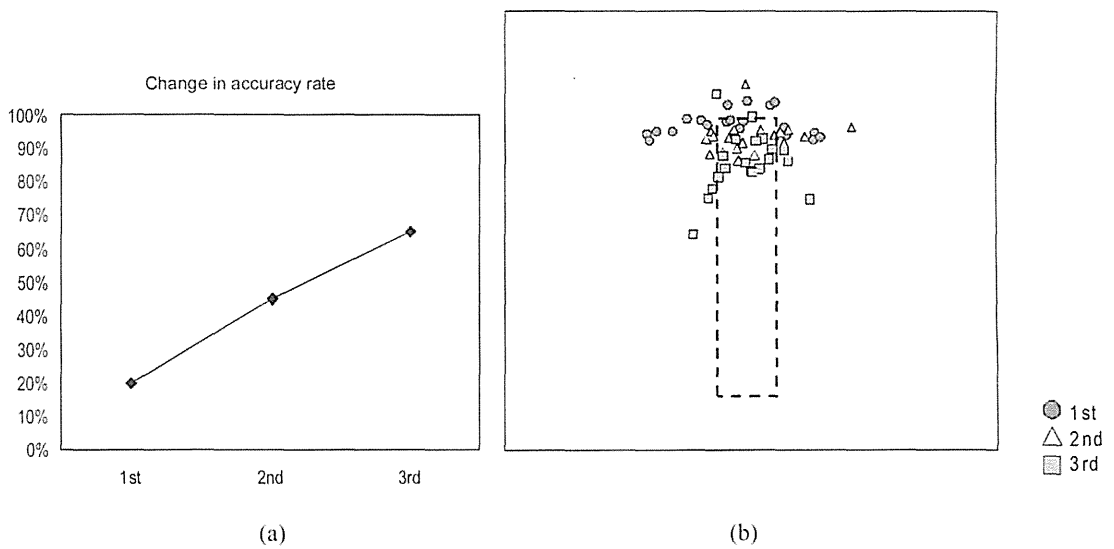

(a)

(b)

Fig. 4. Result of the touch panel display task. (a) Changes in success rates after repetition of examination. (b) Touched positions when the white bar was presented on the display.
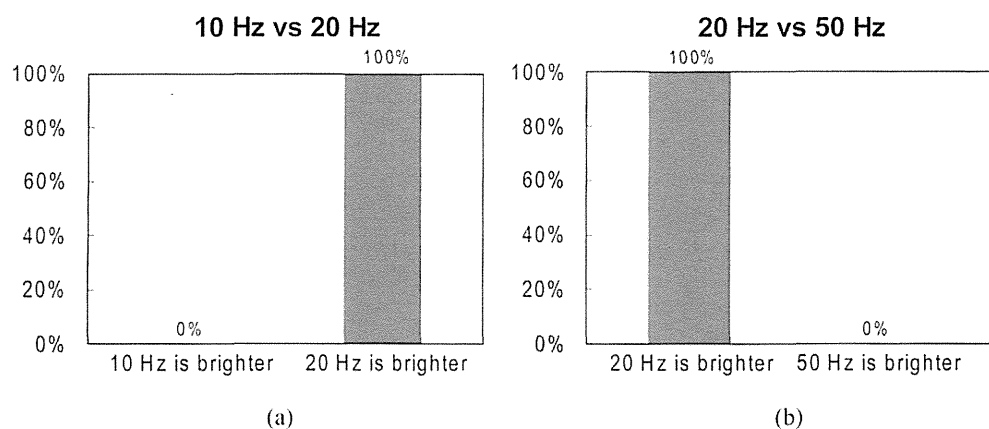
10 Hz vs 20 Hz

20 Hz vs 50 Hz

Fig. 5. Comparison of subjective brightness of phosphene between different pulse frequencies. The patient was asked to state which pulse frequency evoked a brighter phosphene. The trials were repeated 4 times for each parameter set. (a) Comparison between 10 and 20 Hz. (b) Comparison between 20 and 50 Hz.

electrodes. The success rate of identifying a white bar on the touch panel increased after repeated testing. It suggests that a training effect may have occurred during the testing. Chronic implantation of the electrode array-STS system showed that our approach for retinal prosthesis is safe and feasible for artificial vision. Further improvements are necessary to achieve reading ability, and this may require increasing the number of functional electrodes.

References

1   R. A. Pagon: Surv. Ophthalmol. **33** (1988) 137.
2   E. Zrenner, K. U. Bartz-Schmidt, H. Benav, D. Besch, A. Bruckmann, V. P. Gabel, F. Gekeler, U. Greppmaier, A. Harscher, S. Kibbel, J. Koch, A. Kusnyerik, T. Peters, K. Stingl, H. Sachs, A. Stett, P. Szurman, B. Wilhelm and R. Wilke: Proc. Biol. Sci. **278** (2011) 1489.
3   M. S. Humayun, J. D. Weiland, G. Y. Fujii, R. Greenberg, R. Williamson, J. Little, B. Mech, V. Cimmarusti, G. Van Boemel, G. Dagnelie and E. de Juan: Vision Res. **43** (2003) 2573.
4   H. Kanda, T. Morimoto, T. Fujikado, Y. Tano, Y. Fukuda and H. Sawai: Invest. Ophthalmol. Vis. Sci. **45** (2004) 560.
5   K. Nakauchi, T. Fujikado, H. Kanda, T. Morimoto, J. S. Choi, Y. Ikuno, H. Sakaguchi, M. Kamei, M. Ohji, T. Yagi, S. Nishimura, H. Sawai, Y. Fukuda and Y. Tano: Graefes Arch. Clin. Exp. Ophthalmol. **243** (2005) 169.
6   H. Sakaguchi, T. Fujikado, X. Fang, H. Kanda, M. Osanai, K. Nakauchi, Y. Ikuno, M. Kamei, T. Yagi, S. Nishimura, M. Ohji, T. Yagi and Y. Tano: Jpn. J. Ophthalmol. **48** (2004) 256.
7   T. Fujikado, T. Morimoto, H. Kanda, S. Kusaka, K. Nakauchi, M. Ozawa, K. Matsushita, H. Sakaguchi, Y. Ikuno, M. Kamei and Y. Tano: Graefe's Arch. Clin. Exp. Ophthalmol. **245** (2007) 1411.

ORIGINAL ARTICLE

Implantation of a newly developed direct optic nerve electrode device for artificial vision in rabbits

Hirokazu Sakaguchi · Motohiro Kamei · Kentaro Nishida ·
Yasuo Terasawa · Takashi Fujikado · Motoki Ozawa ·
Kohji Nishida

Abstract The purpose of this study was to investigate the surgical procedures involved in the implantation of a newly developed direct optic nerve electrode device for inducing artificial vision. The electrode device comprised seven wire stimulation electrodes and a return electrode (diameter 50 μm), one manipulation rod (diameter 100 μm), and a cylindrical silicone board (diameter 2.0 mm). The stimulation electrodes and the manipulation rod protruded through the board to allow implantation of the electrode tips into the optic disc of the rabbit eye. The surgical procedures required to insert the device into the vitreous cavity and implant the device into the optic disc were evaluated. When the electrodes were stimulated, electrically evoked potentials (EEPs) were recorded at the visual cortex. The electrode device was inserted into the vitreous cavity with no damage using a trocar through a scleral incision. The device was easily manipulated using vitreoretinal forceps in the vitreous cavity, and the electrode tips were implanted into the optic disc in a single insertion after vitrectomy. When electrical stimulation was applied, EEPs were recorded from all electrode pairs. The newly developed electrode device was inserted into the eye and implanted into the optic nerve disc smoothly and safely, suggesting that these surgical procedures are useful for our artificial vision system.

Keywords Optic nerve electrode · Electrical stimulation · Electrically evoked potential · Artificial vision

Introduction

Many groups have attempted to develop a visual prosthesis, because no treatment can restore vision lost as a result of retinitis pigmentosa (RP), for example. The targets of electrical stimulation in visual prosthetic systems are the visual cortex, optic nerve, or retina [1–22].

Our group has tried to develop two types of visual prostheses with two different stimulation targets. One type is artificial vision via stimulation using a direct optic nerve electrode (AV-DONE), which targets the optic nerve fibers [19–22]. Another type is the suprachoroidal transretinal stimulation (STS) system [13–17], which is a type of retinal prosthesis. We have performed clinical trials of both systems [15, 17, 22].

Two patients have undergone semi-chronic implantation of the STS system [17]. The internal devices were implanted under the skin on the temporal side of the head, and the 49-electrode array was implanted in a scleral pocket. Phosphenes were elicited by currents delivered through six of nine electrodes in patient 1 and through four of nine electrodes in patient 2.

With the AV-DONE system, after vitrectomy, three linear-shaped electrodes were implanted directly into the

H. Sakaguchi (✉) · M. Kamei (✉) · Kentaro Nishida ·
Kohji Nishida
Department of Ophthalmology, Osaka University Graduate
School of Medicine, 2-2 Yamadaoka, E-7, Suita,
Osaka 565-0871, Japan
e-mail: sakaguh@ophthal.med.osaka-u.ac.jp

M. Kamei
e-mail: mkamei@ophthal.med.osaka-u.ac.jp

Y. Terasawa · M. Ozawa
NIDEK Co., Ltd., 34-14 Maehama, Hiroishi-cho,
Gamagori, Aichi 443-0038, Japan

T. Fujikado
Department of Applied Visual Science,
Osaka University Graduate School of Medicine,
2-2 Yamadaoka, G-4, Suita, Osaka 565-0871, Japan

optic nerve disc of a patient who was blind as a result of RP [22]. When electrical stimulation was applied to the optic nerve fibers through the electrodes, the patient recognized the phosphenes. Moreover, the areas of the phosphenes from each electrode were localized, and the areas changed when different electrodes provided the electrical stimulation. The results suggested that this system might lead to the development of a useful visual prosthetic system.

Our procedure to implant linear-shaped electrodes into the optic disc one by one needs to be improved. The electrode that was inserted into the optic nerve disc became dislodged easily during surgery and required several repeated insertions because the optic disc area was small (diameter ~ 1.8 mm), the electrode wires became entangled, and the wires recoiled. The total time for the implantation session exceeded 1 h.

To solve these problems, we developed a new device comprising seven stimulation electrodes and one reference electrode coated with polytetrafluoroethylene (PTFE, Teflon) that was designed to facilitate one-step implantation of the electrode tips into the optic disc. Teflon is less tough and is easier to use than Parylene, which had been used previously to coat the wires [22]. We confirmed the biocompatibility and durability of Teflon-coated platinum–iridium wires in animal eyes [23].

In the current animal study, we developed surgical procedures to implant the new electrode device and investigate the efficacy of this device in animals.

Methods

A new direct optic nerve electrode device

The electrode device comprised seven stimulation electrodes, a return electrode, one rod for manipulation and fixation, and a cylindrical silicone board (Fig. 1).

All electrodes were made of PTFE-coated platinum–iridium wires (90 % platinum and 10 % iridium) of diameter 50 μm; the insulation was 9 μm thick (Goodfellow Cambridge Ltd., Huntingdon, UK). The rod was a platinum–iridium bar (diameter 100 μm) made of 80 % platinum and 20 % iridium (Goodfellow Cambridge Ltd.). The diameter of the cylindrical silicone board was 2.0 mm (Fig. 1).

One millimeter of each stimulation electrode and 3 mm of the manipulation rod protruded through the silicone board. The top of the return electrode terminated in the middle of the silicone board. A 0.5 mm segment of the active tip of each of the stimulation and return electrodes was left uncoated. All wires were aligned parallel to each other.

The PTEE-coated platinum–iridium wires following the cylindrical silicone board were coated with a silicon tube
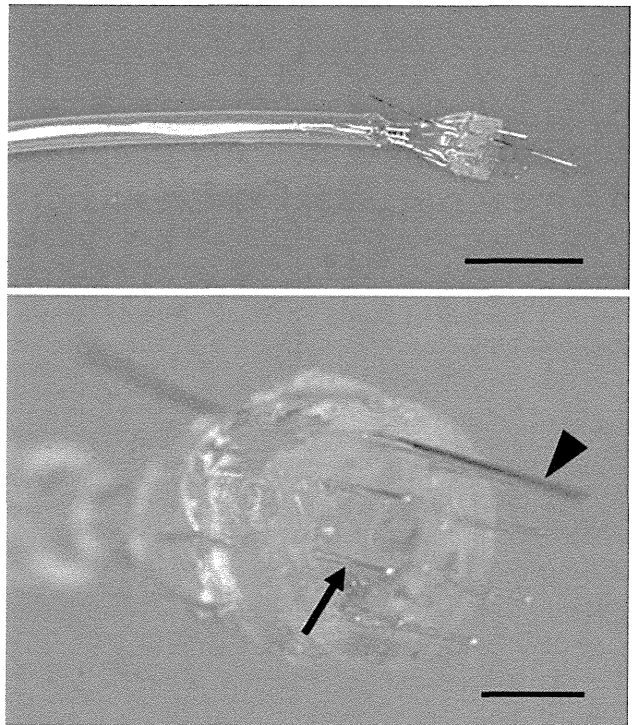

Fig. 1 The electrode device. *Upper:* this device comprises seven stimulation electrodes, one return electrode, one rod, and a cylindrical silicone board. The electrodes are made of PTFE (Teflon)-coated platinum–iridium wires with a diameter of 50 μm and an insulation thickness of 9 μm. The rod is a platinum–iridium wire 100 μm in diameter. The diameter of the cylindrical silicone board is 2.0 mm. *Scale bar* 3 mm. *Lower:* a magnified image shows the tip of the device. The electrode wires protrude through the board. The *arrow* indicates a stimulation electrode and the *arrowhead* indicates the manipulation rod. A small segment (0.5 mm) of the active tip of each stimulation electrode is uncoated. The wires are parallel to each other. *Scale bar* 1 mm

(Silascon®, Kaneka Medix Corp., Tokyo, Japan), with inside and outside diameters of 0.50 and 1.0 mm, respectively.

Surgical procedures to implant the electrode device

We first used four enucleated pig eyes to design the surgical procedures for inserting the device into the vitreous cavity. After a scleral incision had been created, the electrode device was inserted into the vitreous cavity. A 20-mm-long Teflon tube (AWG-11, Chukoh Chemical Industries, Ltd., Tokyo, Japan) with inside and outside diameters of 2.41 and 3.01 mm, respectively, was used as a trocar to insert the device.

We then used three Japanese albino rabbits (4–6 months old) weighing 2–2.5 kg to confirm the implantation procedure. The rabbits were purchased from a vendor (Hokusetsu, Setsu, Osaka, Japan). No rabbits had retinal diseases before the study. All experiments were performed